# Chapter 5
# Mechanical Behavior of Nanowires with High-Order Surface Stress Effects

**Min-Sen Chiu and Tungyang Chen**

**Abstract** Surface in solids could behave differently from their bulk part, especially when the size of the solid is on the nanoscale. It has been widely accepted that the continuum mechanics framework along with a suitable implementation of the surface effect, referred to as surface stress model, could serve as a useful tool in the analysis of mechanical behavior of nanosized solids and structures. Here we review the surface stress model briefly and outline recent progress in application to mechanics of nanosolids or nanocomposites. A refined model, termed high-order surface stress model proposed by the authors few years ago, was recapitulated here, particularly for two-dimensional configurations. The distinction between the two frameworks is highlighted from the viewpoint of a simple geometric exposition of mechanics of thin plate and shell. We demonstrate that, by comparison with experimental data, the incorporation of high-order surface stress could be critical in certain situations to capture the trend observed by the experimental observation. Some illustrations are directed to the mechanics of nanowires, including bending and bulking behavior. Future potential subjects along the trend are suggested.

## 5.1 Introduction

For nanostructures or nanoscaled solids, due to their large specific surface-to-volume ratio, surface effects play an important role on the size-dependent physical properties. The subject of surface elasticity, incorporating surface stress effects, has received considerable attention in the last decade. This effect is particularly important for nanosized solids and composites in that they possess large specific surface area. The concept of surface tension in fluids dates back to more than about two centuries ago by the celebrated Young-Laplace (YL) equation (Young 1805; Laplace 1806). Surface tension in fluids is defined as a force per unit length along the perimeter of the interface. Surface stress in solids seems to be first introduced by Gibbs (1928), which is defined through the change in excess free energy when

M.-S. Chiu • T. Chen (✉)
Department of Civil Engineering, National Cheng Kung University, Tainan, 70101 Taiwan
e-mail: visquel88@hotmail.com; tchen@mail.ncku.edu.tw



S.A. Meguid, G.J. Weng (eds.), *Micromechanics and Nanomechanics of Composite Solids*, DOI 10.1007/978-3-319-52794-9_5

the interface is deformed at constant referential area. In contrast to fluids, surface stress may not be isotropic and may depend on the crystallographic parameters of the solids jointed at the interface. This stress is caused by the differences in configuration and in coordination numbers between atoms at the surface and in the bulk. In addition to surface of the domain boundary, surface effects also exist in interfaces between different regions, such as inclusions and the surrounding matrix. Interface stress is also playing the same role as that of surface stress. Using an atomistic calculation analysis, Zhou and Huang (2004) demonstrated that a solid surface can be either elastically softer or stiffer than their bulk counterparts. This surface effect phenomenon has been studied in different disciplines, ranging from material science, physical chemistry, to continuum mechanics (e.g., Nix and Gao 1998; Miller and Shenoy 2000; Thomson et al. 1986; Spaepen 2000; Duan et al. 2005a, b, c; Chen and Dvorak 2006). The aim of this chapter is to give an introductory exposition of the subject and to summarize our recent proposition for the high-order surface stress model, with potential applications in various problems of nanosized solid and composites.

Specifically, we see in this chapter how the high-order surface stress model will influence the solutions significantly for certain boundary value problems. The size-dependent mechanical behavior of nanowires (NWs) will be demonstrated. The difference between the calculations based on the high-order surface stress model and the Gurtin-Murdoch model can be seen remarkably, especially when the scale is in a few nanometers. This framework provides a simple continuum mechanics approach, in place of atomistic analysis or experiments, to analyze the mechanical behavior of nanostructures in a refined manner.

## 5.2 Surface Stresses in Mathematical Descriptions

It is generally thought that the surface stress tensor, $\sigma^s_{\alpha\beta}$, is connected to the deformation-dependent surface energy by the relation $\sigma^s_{\alpha\beta} = \tau^0\delta_{\alpha\beta} + \partial G/\partial\varepsilon^s_{\alpha\beta}$ (Shuttleworth 1950; Cammarata 1994). $\tau^0$ and $\varepsilon^s_{\alpha\beta}$ denote the constant residual surface tension and the strain tensor for surfaces, respectively, and $\delta_{\alpha\beta}$ is the Kronecker delta for surfaces. The Greek indices take on values of interfacial components, taking the numbers of 1–2, while the Latin index numbers indicated later will range from 1 to 3. The index 3 will designate the normal direction of the interface. The interface stresses can be written as a linear constitutive law, $\sigma^s_{\alpha\beta} = \tau^0\delta_{\alpha\beta} + L_{\alpha\beta\gamma\delta}\varepsilon^s_{\gamma\delta}$ (Miller and Shenoy 2000), in which $L_{\alpha\beta\gamma\delta}$ stands for the surface stiffness tensor. Considering isotropic surface property, the linear relationship between surface stress tensor $\sigma^s_{\alpha\beta}$ and surface strain field can be written in the form (Gurtin and Murdoch 1975, 1978; Assadi et al. 2010) $\sigma^s_{\alpha\beta} = \tau^0\delta_{\alpha\beta} + (\mu_s - \tau^0)\left(u^s_{\alpha,\beta} + u^s_{\beta,\alpha}\right) + (\lambda_s + \tau^0)\,u^s_{\gamma,\gamma}\delta_{\alpha\beta} + \tau^0 u^s_{\alpha,\beta}$. In the exposition, $u^s_\alpha$ are the displacement components of the surface, while $\lambda_s$ and $\mu_s$ are surface Lame constants. The effect of residual tension $\tau^0$ is not associated with the deformation

and is sometimes ignored in some relevant studies. For example, Sharma et al. (2003) investigated the elastic state of eigenstrained spherical inhomogeneities with surface effects and interpreted the concentration factor as a function of surface properties and void radius. Sharma and Ganti (2004) presented closed-form expressions of the modified Eshelby's tensor for spherical and cylindrical inclusions incorporating surface effects. Nix and Gao (1998) employed a simple spring model to calculate the excess free energy of interface atoms. They pointed out that this microscopic model is in complete accord with the classical macroscopic interpretation for interface stresses (i.e., $\sigma^s_{\alpha\beta} = \tau^0\delta_{\alpha\beta} + \partial G/\partial\varepsilon^s_{\alpha\beta}$). Gurtin and Murdoch (1975), in their 1975 paper, derived a mathematical framework for an interface between two different solids with interface stresses using the classical membrane theory (see also Gurtin and Murdoch 1978; Landau and Lifshitz 1987; Povstenko 1993; Gurtin et al. 1998; Chen et al. 2006; Ru 2010 for subsequent developments). In the formulation, a surface is assumed to ideally adhere to its counterpart bulk and modeled as a layer of vanishing thickness. This condition was referred to as the generalized Young-Laplace (generalized YL) equation in distinction with its counterpart in fluids. Chen et al. (2006) presented a simple geometrical exposition for the generalized YL equations, which provide a better description on the underlying physical meaning of the YL equation in solids. This approach is based on the notion that the interface stresses can be modeled as in-plane stresses along the tangential planes of the curved surface and the stress vectors on the top and lower faces of the curved surfaces are contributed from its three-dimensional bulk neighborhood. The generalized YL equations were also derived with generally curvilinear coordinates (Weng and Chen 2010), which are better suited for descriptions of some nanostructures, such as nanotubes, in which the grids are not orthonormal.

The modeling of surface/interface stress can be simulated by introducing a vanishingly thin interphase layer between two different regions with relatively high stiffness compared with the adjacent phases. A general rigorous approach is to resolve the elasticity solution for a three-phase configuration and then deduce to a two-phase one through a deliberated asymptotic process. A schematic illustration of the approach is demonstrated in Fig. 5.1. This approach allows us to effectively replace the effect of the thin interphase by equivalent interface conditions without having to resolve the fields within the interphase. Benveniste and Miloh (2001) examined the effects of imperfect soft and stiff interfaces in two-dimensional elasticity. Based on an asymptotic analysis, they showed that, depending on the softness or stiffness of the interphase layer with respect to the neighboring media, there exist seven regimes of interface conditions.

Other derivations can be found in Benveniste (2006a, b) for a three-dimensional thin interphase with anisotropic properties in elasticity as well as higher-order effects in conduction phenomenon. However, all these developments, based on rigorous asymptotic analysis, are indeed mathematically complicated. In summary, the conventional surface stress model is generally referred to as "generalized Young-Laplace (YL) equation," "Gurtin-Murdoch model," or "an $O(h^N)$ interface model with $N = 1$" (Benveniste 2006a, b), i.e., "first-order interface condition" where $h$ is

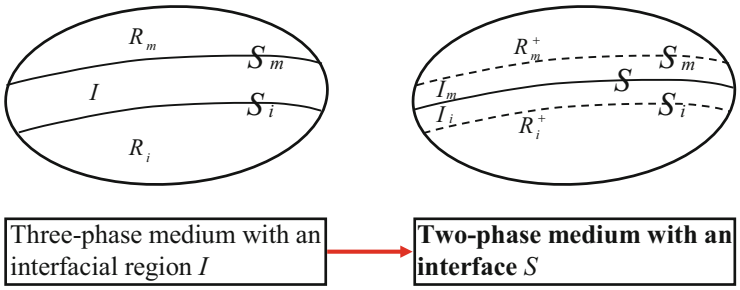


**Fig. 5.1** Surface stress along the interface can be modeled by a thin interphase degenerated into an infinitesimal thickness

the thickness of the interphase layer. Interface or surface stresses incorporating high-order effects may be designated as "an $O(h^N)$ interface model with $N>2$" in which $N$ is an integer. Other relevant researches in this category include Shuttleworth (1950), Bövik (1994), Benveniste and Baum (2007), Ting (2007), and Benveniste and Berdichevsky (2010).

In the following, we introduce some analysis and other aspects of applications related to one-dimensional mechanics problems within the generalized YL model. Nanowires are typical and important nanostructures in sensors, actuators, opto-electronics, and nanoelectromechanical systems (Wang 2009). The size-dependent overall mechanical behavior of NWs has been experimentally observed (Song et al. 2005; Jing et al. 2006; Ni and Li 2006; Ji et al. 2007; Young et al. 2007; Zhu et al. 2009) and theoretically demonstrated based on the Gurtin-Murdoch model (Wang and Feng 2007; He and Lilley 2008a, b; Wang and Feng 2009a, b; Abbasion et al. 2009; Wang and Feng 2010; Jiang and Yan 2010; Farshi et al. 2010; Wang and Yang 2011; Wang and Wang 2011; Yan and Jiang 2011a, b; He and Lilley 2012; Samaei et al. 2012; Zhang et al. 2013; Gao 2015). Considering the first-order interface condition, the stress jump $\bigtriangleup\sigma_{ij}$ across an interface surface is associated with the curvature tensor $\kappa_{\alpha\beta}$ of the surface by the relationship $\triangle\sigma_{ij}n_in_j = \sigma^s_{\alpha\beta}\kappa_{\alpha\beta}$ $(i,j=1,\ 2,\ 3;\ \alpha,\ \beta=1,\ 2)$ in which $n_i$ is the unit vector normal to the interface surface and $\sigma^s_{\alpha\beta}$ is the interface (surface) stress tensor. In one-dimensional problems, the surface constitutive relation $\sigma^s_{\alpha\beta} = \tau^0_{\alpha\beta} + S_{\alpha\beta\gamma\delta}\varepsilon^s_{\alpha\beta}$ can be simplified as $\sigma^s = \tau^0 + E_s\varepsilon^s$ within the framework of Gurtin-Murdoch model, where $\sigma^s$ is the surface stress, $\varepsilon^s$ is the surface strain, $E_s$ is the effective surface Young's modulus, and $\tau^0$ is the constant residual surface tension. For the developments in this line, Wang and Feng (2007) examined the natural frequency of microbeams with surface effect. Wang and Feng (2009a) derived the analytical relation for the axial buckling force of a nanowire under consideration of surface elasticity and residual surface tension effects. The dependence of the surface effects on the overall Young's modulus of bending nanowires in static and resonance has been studied by He and Lilley (2008a, b) for three different boundary conditions. In addition to Euler-Bernoulli beam theory, Timoshenko beam model has also been utilized to investigate the surface effects on the buckling (Wang and Feng 2009b) and free vibration behavior of a nanowire (Wang and Feng 2009b; Abbasion et al. 2009).

Recently, Jiang and Yan (2010) derived explicit solutions for studying the combined effects of shear deformation, surface elasticity, and residual surface tension on the effective stiffness via Timoshenko beam theory as well. It was found that the derivations in some of the above-mentioned one-dimensional researches agree with the experimental measurements well (Lachut and Sader 2007).

## 5.3 High-Order Surface Stresses in Two-Dimensional Configuration

A refined surface stress model, referred to as high-order surface stress model, was recently proposed by the authors (Chen and Chiu 2011). A schematic diagram for the difference between the higher-order interface stress model and the conventional surface stress model is illustrated in Fig. 5.2. For convenience, the concept is illustrated for a two-dimensional configuration. For the conventional surface stress model, only the in-plane surface/interface stress $\sigma_\alpha^s$ is considered in the force balance consideration. While for the high-order surface stress model, in addition to in-plane surface/interface stress $\sigma_\alpha^s$, the surface moment $m_\alpha^s$ is considered at the same time. The surface moment can be viewed as the effect of nonuniformity of the in-plane surface/interface stress across the thickness $h_1$ of the interphase (Fig. 5.2). The approach to introduce $\sigma_\alpha^s$ and $m_\alpha^s$ into the continuum framework is somewhat akin to the classical theories of beams, thin plates, and shells. As shown in Fig. 5.2,

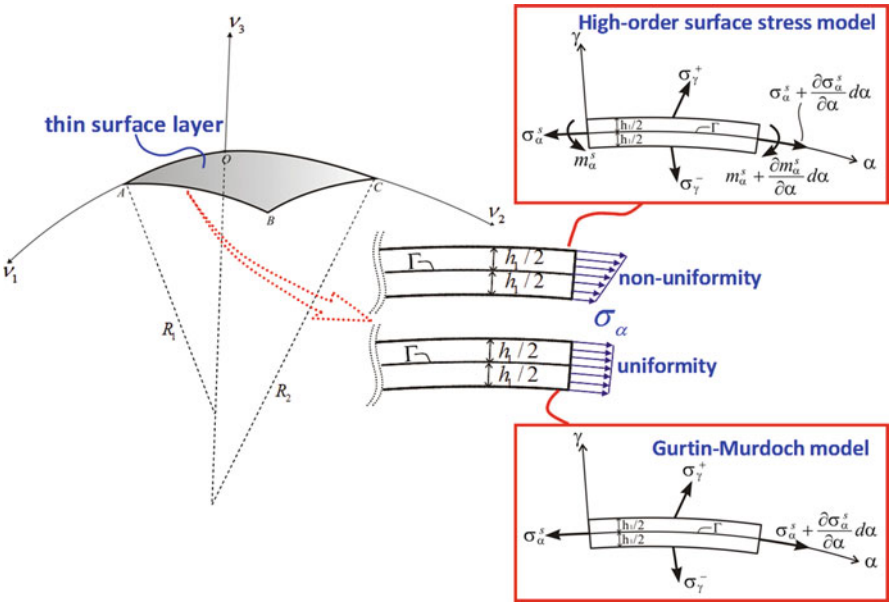


**Fig. 5.2** A schematic illustration of two different surface stress models in two-dimensional configurations: high-order surface stress model and Gurtin-Murdoch model

the stresses $\sigma_\alpha$ along the in-plane direction ($\alpha$-direction) of the layer are replaced by statically equivalent stress resultants and stress moments through the relations $\sigma_\alpha^s = \int_{-h_1/2}^{h_1/2} \sigma_{\alpha\alpha}\ d\gamma, m_\alpha^s = \int_{-h_1/2}^{h_1/2} \sigma_{\alpha\alpha}\gamma\ d\gamma$, and then they are interpreted as surface stress $\sigma_\alpha^s$ and surface moment $m_\alpha^s$, respectively. Of course, when only the in-place surface stress is considered and the effect of $m_\alpha^s$ is omitted from the beginning, this will reduce to the conventional surface stress model based on the membrane theory (generalized YL equation) (Chen et al. 2006).

For the kinematic deformation of the infinitesimally thin layer, based on the Kirchhoff-Love theory of thin shell, the relations were constructed as $\sigma_\alpha^s = E_s\varepsilon_\alpha^0$, $m_\alpha^s = -D_s\kappa_\alpha^0$. We mention that $\varepsilon_\alpha^0$ and $\kappa_\alpha^0$ are, respectively, the strain and the change in curvature on the middle surface of the thin layer. $E_s$ is the surface Young's modulus, defined as $E_s = E_c h_1/(1-\nu_c{}^2)$ here. It is equivalent to the material parameters $\lambda_s + 2\mu_s$ defined in Chen et al. (2007a, b). Note that $h_1$, $E_c$, and $\nu_c$ are the thickness, Young's modulus, and Poisson's ratio of the thin layer, respectively. On the other hand, $D_s$ is the flexure rigidity of the thin surface/interface layer, defined as $D_s = E_c h_1^3/12/\left(1-\nu_c{}^2\right)$.

When the thin layer has a high stiffness compared to its neighboring phases, the effective behavior of the layer can be viewed as a stiff interface. When the stiffness of the thin layer is with magnitudes of high orders $O(h^{-N})$, various kinds of interface conditions can be developed. In addition to the continuity condition for the displacements, $u_\alpha^{(i)}\Big|_\Gamma = u_\alpha^{(m)}\Big|_\Gamma$ and $u_\gamma^{(f)}\Big|_\Gamma = u_\gamma^{(m)}\Big|_\Gamma$, the jump conditions in traction would characterize different degrees of stiff interfaces. These include four types of interface conditions (Benveniste and Miloh 2001; Chen and Chiu 2011).

I. Perfectly bonded interfaces

$$\left[\sigma_{\gamma\alpha}\right]_\Gamma = \left[\sigma_{\gamma\gamma}\right]_\Gamma = 0. \tag{5.1}$$

II. Membrane type interface (the generalized YL equation)

$$\left[\sigma_{\gamma\alpha}\right]_\Gamma = -\left(\frac{\partial\sigma_\alpha^s}{\partial s}\right)_\Gamma, \qquad \left[\sigma_{\gamma\gamma}\right]_\Gamma = -\left(\frac{\sigma_\alpha^s}{R}\right)_\Gamma. \tag{5.2}$$

III. Inextensible membrane type

$$\begin{aligned} &\varepsilon_\alpha^0 = \left.\frac{\partial u_\alpha^0}{\partial s} - \frac{u_\gamma^0}{R}\right|_\Gamma = 0, \\ &\left[\sigma_{\gamma\alpha}\right]_\Gamma - \frac{\partial}{\partial s}\left\{R\left[\sigma_{\gamma\gamma}\right]_\Gamma\right\} = 0. \end{aligned} \tag{5.3}$$

IV. Inextensible classical shell type

$$\begin{aligned} &\varepsilon_\alpha^0 = \left.\frac{\partial u_\alpha^0}{\partial s} - \frac{u_\gamma^0}{R}\right|_\Gamma = 0, \\ &\left[\sigma_{\gamma\alpha}\right]_\Gamma - \frac{\partial}{\partial s}\left\{R\left[\sigma_{\gamma\gamma}\right]_\Gamma\right\} = \left(\frac{1}{R}\frac{\partial m_\alpha^s}{\partial\alpha}\right)_\Gamma + \frac{\partial}{\partial s}\left\{R\frac{\partial^2 m_\alpha^s}{\partial s^2}\right\}. \end{aligned} \tag{5.4}$$

We mention that Type I is the classical perfectly bonded condition and Type II is the conventional surface stress model, or the so-called Gurtin-Murdoch model. Types III and IV represent the stiff interface deduced from the high-order surface stress. It is noted that the inextensible condition $\varepsilon_{\alpha}^{0} = 0$ exists in both Type III and IV. These four kinds of interface conditions demonstrate the mathematical behavior of thin interphase layer between two neighboring media

Benveniste and Miloh (2001) derived the generalized interface conditions using an asymptotic expansion method. With the rigorous approach, Types I–IV here and the rigid type interface condition are termed stiff interfaces. In addition, they also derived two different types of soft interfaces.

### 5.3.1 *Boundary Value Problem: A Circular Inclusion in an Infinite Matrix*

We now illustrate the high-order surface effect by considering the boundary value problem of a circular inclusion in an infinite matrix under a transverse shear deformation applied at the remote boundary. The effect of high-order surface stresses is compared with that of simple surface stress model to exemplify the significance of high-order effects in certain situations. We will also see that the surface stress model and the high-order surface stress model both will have size-dependent behavior, depending on the geometric size of the inclusion. In Fig. 5.3, we suppose that the radius of the circular fiber is denoted by $a$. The effects of various types of interface conditions described in Eqs. (5.1)–(5.4) will be considered along the interface between the fiber and the matrix. It was noted that for high-order interface stresses, namely, Types III and IV, the "inextensible" interface condition needs to prevail (Chen and Chiu 2011). Thus, only the asymmetric deformation mode will be considered to examine the effect of high-order interface

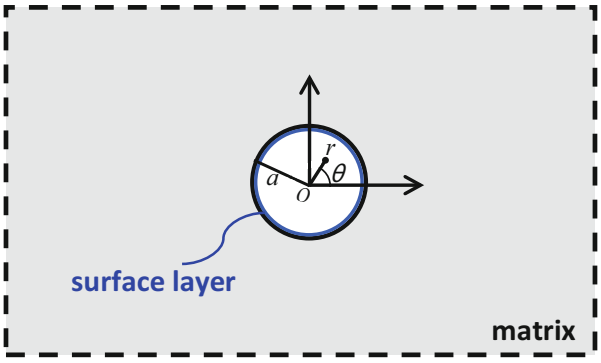


**Fig. 5.3** Schematic illustration of a composite medium composed of the matrix containing circular cavity with radius $a$ under the surface effects resulting from thin surface layer

stresses. The circular cylindrical coordinate is adapted within the mathematical continuum framework. The coordinate variables in Eqs. (5.1)–(5.4) are replaced with $\alpha = \theta$ and $\gamma = r$. Also, in the substitutions of $\partial s = r\partial\theta$ and $1/R = -1/r$, we can obtain the corresponding interface conditions in circular cylindrical coordinate for the present boundary value problem.

As an illustration for high-order interface stress effects, the configuration of a circular cavity in an unbounded isotropic matrix subjected to a remote transverse shear $\sigma_x^m\big|_{r\to\infty} = -\sigma_y^m\big|_{r\to\infty} = \sigma^0$ was studied by Chen and Chiu (2011). The stress concentration factor around the cavity surface was examined. The concentration factor is defined as the ratio of hoop stress on the cavity surface versus the applied stress $\sigma^0$ for the four different types of interfaces. The results were derived in explicit closed forms as

$$\textbf{Type I}: \left.\frac{\sigma_\theta}{\sigma^0}\right|_{r\to a} = -4\cos 2\theta, \tag{5.5}$$

$$\textbf{Type II}: \left.\frac{\sigma_\theta}{\sigma^0}\right|_{r\to a} = -\frac{4km + (E_s/a)(k-m)}{km + (E_s/2a)(2k+m)}\cos 2\theta, \tag{5.6}$$

$$\textbf{Type III}: \left.\frac{\sigma_\theta}{\sigma^0}\right|_{r\to a} = -\frac{2(k-m)}{2k+m}\cos 2\theta, \tag{5.7}$$

$$\textbf{Type IV}: \left.\frac{\sigma_\theta}{\sigma^0}\right|_{r\to a} = \frac{-2m(k-m) + 12\left(D_s/a^3\right)(k-m)}{m(2k+m) + 6\left(D_s/a^3\right)(k+2m)}\cos 2\theta. \tag{5.8}$$

We mention that the stress concentration factor for Type I is exactly the result of perfectly bonded interface given in Timoshenko and Goodier (1970) and that of Type II is identical with the surface stress model previously derived by Chen et al. (2007a). When letting $E_s/a \to 0$ in (5.6), Eq. (5.6) for Type II will reduce to the classical elasticity solution with a concentration factor of $-4$. On the other hand, when $E_s/a$ is a relatively large quantity compared with the orders of $k$ and $m$, then the concentration factor of Eq. (5.6) will approach to Eq. (5.7) for Type III. In addition, in Eq. (5.8), when one has $D_s/a^3 \to 0$, the concentration factor will reduce to that of Eq. (5.7) for Type III. Also, when $D_s/a^3$ is a large quantity compared with other terms in the numerator and denominator of Eq. (5.8), the expression of Eq. (5.8) will reduce to the result of an infinite medium containing a rigid inclusion. We mention that these four types of interface conditions characterize the degree of "stiffness" from the ideal situation (Type I) to the nearly rigid interface (Type IV) in a successive manner (Chen and Chiu 2011).

The stress concentration factor for stress components $\sigma_r$ and $\sigma_{r\theta}$ of an infinite medium containing a circular cavity under different types of interface conditions can also be derived as

$$\textbf{Type I}: \quad \left.\frac{\sigma_r}{\sigma^0}\right|_{r\to a} = 0, \tag{5.9}$$

$$\textbf{Type II}: \quad \left.\frac{\sigma_r}{\sigma^0}\right|_{r\to a} = -\frac{(E_s/a)\,(k+m)}{km + (E_s/2a)\,(2k+m)}\cos 2\theta, \tag{5.10}$$

$$\textbf{Type III}: \quad \left.\frac{\sigma_r}{\sigma^0}\right|_{r\to a} = -\frac{2\,(k+m)}{2k+m}\cos 2\theta, \tag{5.11}$$

$$\textbf{Type IV}: \quad \left.\frac{\sigma_r}{\sigma^0}\right|_{r\to a} = \frac{-2m\,(k+m) + 12\left(D_s/a^3\right)(k+m)}{m\,(2k+m) + 6\,(D_s/a^3)\,(k+2m)}\cos 2\theta, \tag{5.12}$$

$$\text{rigid inclusion}: \quad \left.\frac{\sigma_r}{\sigma^0}\right|_{r\to a} = \frac{2\,(k+m)}{k+2m}\cos 2\theta, \tag{5.13}$$

for the radial stress $\sigma_r$ and

$$\textbf{Type I}: \quad \left.\frac{\sigma_{r\theta}}{\sigma^0}\right|_{r\to a} = 0, \tag{5.14}$$

$$\textbf{Type II}: \quad \left.\frac{\sigma_{r\theta}}{\sigma^0}\right|_{r\to a} = -\frac{2\,(E_s/a)\,(k+m)}{km + (E_s/2a)\,(2k+m)}\sin 2\theta, \tag{5.15}$$

$$\textbf{Type III}: \quad \left.\frac{\sigma_{r\theta}}{\sigma^0}\right|_{r\to a} = -\frac{4\,(k+m)}{2k+m}\sin 2\theta, \tag{5.16}$$

$$\textbf{Type IV}: \quad \left.\frac{\sigma_{r\theta}}{\sigma^0}\right|_{r\to a} = -\frac{4m\,(k+m) + 12\left(D_s/a^3\right)(k+m)}{m\,(2k+m) + 6\,(D_s/a^3)\,(k+2m)}\sin 2\theta, \tag{5.17}$$

$$\text{rigid inclusion}: \quad \left.\frac{\sigma_{r\theta}}{\sigma^0}\right|_{r\to a} = -\frac{2\,(k+m)}{k+2m}\sin 2\theta, \tag{5.18}$$

for the shear stress $\sigma_{r\theta}$. As in the hoop stress $\sigma_\theta$, we see that Eqs. (5.9)–(5.13) for $\sigma_r$ and Eqs. (5.14)–(5.18) for $\sigma_{r\theta}$ also show that these four types of interface conditions characterize the degree of "stiffness" from the ideal situation (Type I) to the nearly rigid interface (Type IV) in a successive manner. Note that here $k_m$ and $m_m$ have been written simply by $k$ and $m$ for simplicity.

## 5.4 High-Order Surface Stresses in Nanowires

In this section, we present the high-order surface stress effect on the mechanical behavior of nanowires. Specifically, the high-order surface stress model developed in Sect. 5.3 was implemented for the static bending and buckling behavior of NWs. In line with the previous related references (Wang and Feng 2007; He and Lilley 2008a, b; Wang and Feng 2009a, b), the effect of surface elasticity as well as the

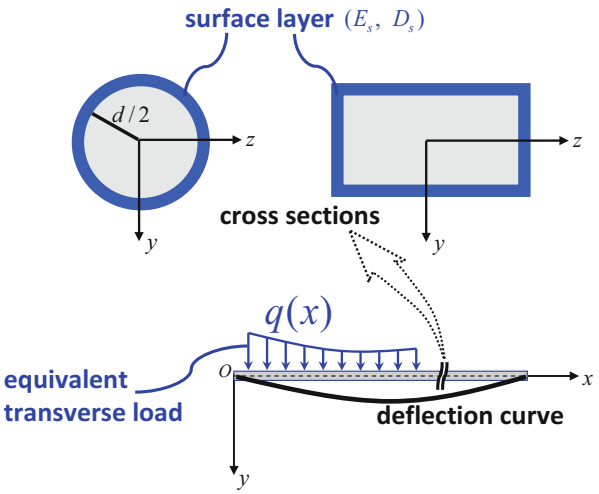


**Fig. 5.4** Cross sections of circular and rectangular nanowires with a surface layer and bending in the $x$ - $y$ plane with equivalent distributed transverse load $q(x)$ resulting from surface moments as well as in-plane surface stresses

effect of residual surface tension will be examined. We compare the present results with previous studies based on the Gurtin-Murdoch model and with the existing experimental data. It is demonstrated that the high-order surface stress effect can be significantly pronounced when the dimension is in a few nanometers.

### 5.4.1 *Mechanical Behavior of NWs Based on Euler-Bernoulli Beam Theory*

In the consideration of residual surface tension $\tau_0$, the linear relations between the surface stress and strain and between the surface moment and curvature can be expressed as $\sigma_\alpha^s = \tau_0 + E_s\varepsilon_\alpha^0$ and $m_\alpha^s = -D_s\kappa_\alpha^0$. We mention that $E_s$ is the surface Young's modulus with the dimensions of N/m and $D_s$ is the surface bending stiffness with the dimensions of Nm. Two different cross-sectional shapes, rectangular and circular cross sections, of NWs were considered (Fig. 5.4). The effect of surface stress, based on the Gurtin-Murdoch model, was simulated by an equivalent distributed transverse force $q(x)$ that acts on the NW in bending (Wang and Feng 2007).

Here, the stress jump for high-order surface stress effect also results in a distributed transverse force (Chiu and Chen 2011a). But the surface stress and surface moment will contribute to different terms in the governing differential equation. For bending NWs in the $y$ direction under small deformation with $\mathrm{v}$ being the NW transverse displacement (Fig. 5.4), the distributed transverse load for NWs with the high-order surface stress effect could be derived as $q(x) = H\mathrm{v}'' - K\mathrm{v}^{(4)}$(Chiu and Chen 2011a), where $\mathrm{v}'' = d^2\mathrm{v}/dx^2$ and $\mathrm{v}^{(4)} = d^4\mathrm{v}/dx^4$. The definitions of $H$ and $K$ can be found in Equation (9) of Chiu and Chen (2011a). For a deformed NW subjected to a compressive force $P$ acting in the longitudinal $x$ direction (Fig. 5.4),

the jump condition resulting from high-order surface stress effect will also give rise to a distributed transverse load $q(x)$ along the NW longitudinal direction. The governing equations based on the high-order surface stress model can be derived as

$$\left[(EI)^* + K\right]\frac{d^4\mathrm{v}}{dx^4} - H_0\frac{d^2\mathrm{v}}{dx^2} = 0 \tag{5.19}$$

for static bending (Chiu and Chen 2011a) and

$$\left[(EI)^* + K\right]\frac{d^4\mathrm{v}}{dx^4} + (P - H_0)\frac{d^2\mathrm{v}}{dx^2} = 0. \tag{5.20}$$

for buckling (Chiu and Chen 2012a). We mention that when neglecting the high-order effect (i.e., $K = 0$), the governing equations in Eqs. (5.19) and (5.20) can be reduced to the corresponding case of static bending (He and Lilley 2008a) and buckling (Wang and Feng 2009a) based on the Gurtin-Murdoch model. Also, when neglecting the surface stress effects (i.e., $K = H_0 = 0$), the results will recover the governing equation of classical beam-column theory (Timoshenko and Gere 1961).

### 5.4.2 *Mechanical Behavior of NWs Based on Timoshenko Beam Theory*

In this section, we will examine the Timoshenko beam (TB) theory incorporating the high-order surface stress effect, in which the shearing deformation could be taken into account. Based on Timoshenko beam theory, the researchers showed that the effect of surface stress within the Gurtin-Murdoch model on the static bending (Jiang and Yan 2010) and buckling (Wang and Feng 2009b) behavior of NWs. Continuing their investigations, the size-dependent buckling (Chiu and Chen 2012b) and static bending (Chiu and Chen 2013) behaviors for NWs based on the high-order surface stress model have been studied. For demonstrations, we record the nondimensional critical compression force (Chiu and Chen 2012b)

$$\frac{P_{cr}}{P_{cr}^0} = \Lambda\left(1 + \frac{6E_s}{Eh} + \frac{2E_s}{Ew} + \frac{24D_s}{Eh^3}\right) + \frac{24}{\eta\pi^2}\frac{\tau_0}{Eh}\left(\frac{L}{h}\right)^2, \tag{5.21}$$

for rectangular sections,

$$\frac{P_{cr}}{P_{cr}^0} = \Lambda\left(1 + \frac{8E_s}{Ed} + \frac{128D_s}{\pi Ed^3}\right) + \frac{128}{\eta\pi^3}\frac{\tau_0}{Ed}\left(\frac{L}{d}\right)^2, \tag{5.22}$$

for circular sections, and the size-dependent effective Young's modulus $E_{\mathrm{eff}}$, based on TB theory was found as

$$E_{\text{eff}} = \frac{\Lambda\left[(EI)^* + K\right]}{I} + \frac{H_0 L^2}{\eta \pi^2 I}. \tag{5.23}$$

Here the definition of the nondimensional parameter $\Lambda$ is (Chiu and Chen 2012b)

$$\Lambda \equiv \frac{\alpha_s GA}{\alpha_s GA + \eta\left(\pi^2/L^2\right)\left[(EI)^* + K\right]}, \tag{5.24}$$

where $G$ is the shear modulus, $A$ is the cross-sectional area of NWs, and $\eta$ is a constant depending on the boundary conditions. It is noted that when neglecting shear deformation ($G \to \infty$) and thus the parameter $\Lambda \to 1$, Eqs. (5.21)–(5.23) will recover the corresponding results of NWs accounting for the high-order surface stress effects based on Euler-Bernoulli beam (EB) theory.

## 5.5 Results and Discussion

### *5.5.1 The Stress Concentration Factor for a Circular Cavity in an Infinite Matrix*

In numerical illustrations, we present analytic solutions for the stress concentration factor in Sect. 5.3. Figure 5.5 shows the maximum value of stress concentration factor for hoop stress $\sigma_\theta$ for different types of interfaces versus the radius $a$ of cavity. Note that the scale of y-axis in the curves of Type I and Type II is different from that of Type III, Type IV, and rigid inclusion. The matrix material is assumed aluminums with the isotropic bulk modulus $K = 75.2$GPa and shear modulus $\mu = 34.7$GPa (Duan et al. 2005b). Note that the relations between elastic constants ($K$, $\mu$) and Hill's moduli ($k$, $m$) are $k = K + \mu/3$ and $m = \mu$ (Hill 1964).

In Figs. 5.6 and 5.7, we also present the maximum value of stress concentration factor for radial stress $\sigma_r$ and shear stress $\sigma_{r\theta}$ shown in Sect. 5.3 versus the radius $a$ of cavities under different types of interfaces. For the numerical calculations in Figs. 5.5, 5.6, and 5.7, the surface material properties for Type II interface conditions on the basis of Gurtin-Murdoch model are considered in two kinds of different free surface properties, $E_s = -8.9465$ N/m for surface A and $E_s = 6.091$ N/m for surface B (Chen et al. 2007a).

For the material parameter $D_s$ of Type IV interface condition which accounts for the high-order surface stress effect, as explained in Chen and Chiu (2011), moderate and reasonable estimated values ranging from $10^2 \times (10^{-18}\text{Nm})$ to $10^4 \times (10^{-18}\text{Nm})$ are adapted for the numerical illustrations.

In Fig. 5.5, we have checked that the numerical results for Type II are the same as that of Chen et al. (2007a), which utilized the Gurtin-Murdoch model based on the variational method to solve this problem. Obviously, we see that the maximum value is size dependent for Type II and Type IV, but not for Type I and Type III. It is

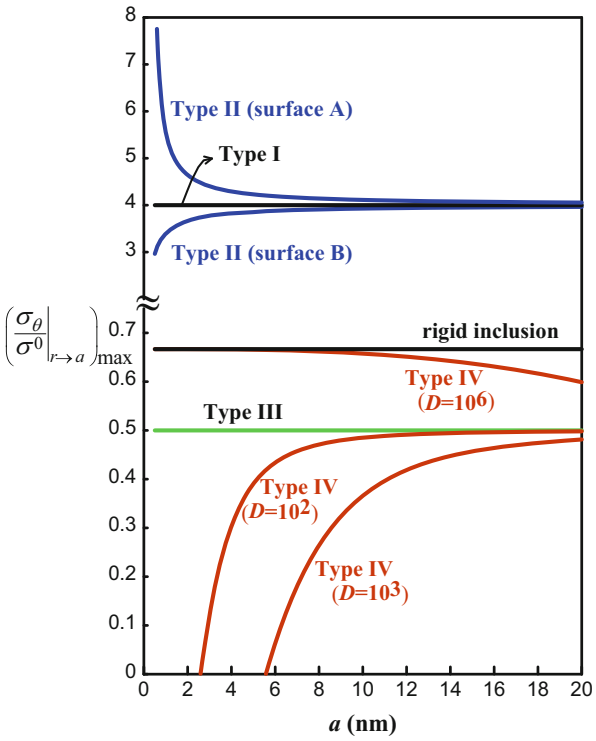


**Fig. 5.5** Maximum value of stress concentration factor for hoop stress $\sigma_\theta$ in different types of interfaces versus the radius $a$ of cavities

interesting to note that the size-dependent behavior for cavity with larger diameter (say $a > 15$ nm) would be still pronounced with the incorporation of high-order surface stress effect (Type IV), while the Type II interface condition has become nearly no size effect.

### 5.5.2 *Mechanical Behavior of NWs*

Figure 5.8 shows the size-dependent effective Young's modulus $E_{\text{eff}}$ numerically. The calculation is based on EB theory incorporating the high-order surface stress effects within the buckling analysis (Chiu and Chen 2012a). We see that the numerical prediction by the theoretical calculation based on the Gurtin-Murdoch model will not be able to capture the general trend of the experimental data, especially when $d \leq 40$ nm. In contrast, the high-order surface stress model will produce a good agreement with the experimental data. This comparison with the experimental data suggests that the effect of surface moments could be crucial in the modeling for mechanical behavior of NWs. In Fig. 5.8, the experimental sample was silicon NWs with fixed-fixed end conditions (Zhu et al. 2009). The surface Young's modulus and residual surface tension were adapted as $E_s = -10.655$N/m and

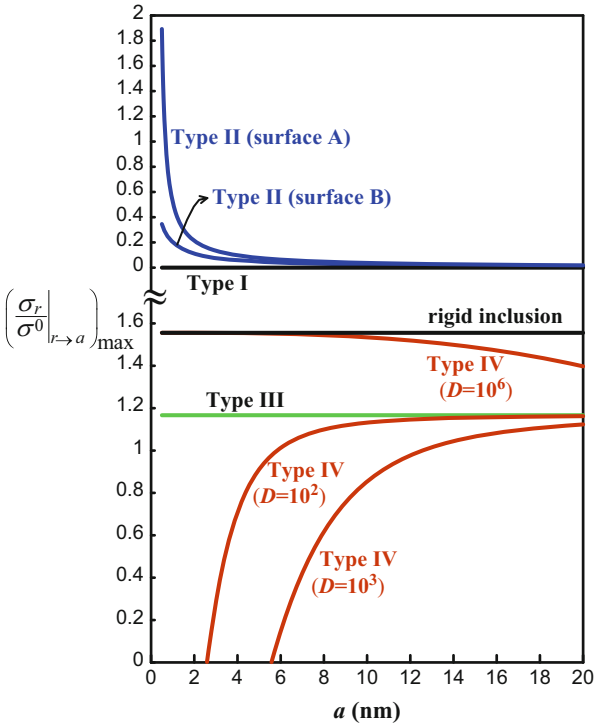


**Fig. 5.6** Maximum value of stress concentration factor for stress component $\sigma_r$ in different types of interfaces versus the radius $a$ of cavity

$\tau_0$=0.6056N/m, respectively (Miller and Shenoy 2000). The high-order material parameter $D_s$ was selected as $D_s=-7\times10^4\times(10^{-18}\text{Nm})$, which has been examined by Chiu and Chen (2012a).

In Fig. 5.9, we demonstrate that the shear deformation of larger NWs, accounting for the framework of TB theory, should not be underestimated. Under the consideration of high-order surface stresses, the size-dependent effective Young's modulus $E_{\text{eff}}$ was theoretically resolved on the basis of static bending analysis (Chiu and Chen 2013). Figure 5.9 presents the numerical solutions of $E_{\text{eff}}$ versus the diameter $d$ for circular NWs. The experimental data in Fig. 5.9 was adapted from Jing et al. (2006), in which fixed-fixed silver NWs were used for observation. We see that when the diameter increases, the solutions considering the shearing effect based on TB theory within the high-order surface stress model will predict more accurate results in comparison with the experimental data than those by EB theory, especially when $d\geq70$ nm. We mention that the material parameter of high-order effect is used as $D_s=5\times10^4\times(10^{-18}\text{Nm})$, which was numerically examined by Chiu and Chen (2013).

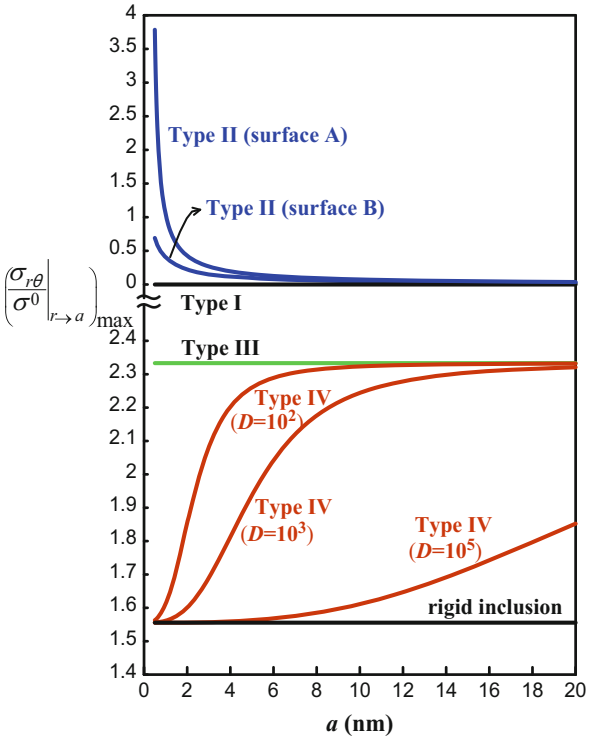


**Fig. 5.7** Maximum value of stress concentration factor for stress component $\sigma_{r\theta}$ in different types of interfaces versus the radius $a$ of cavity

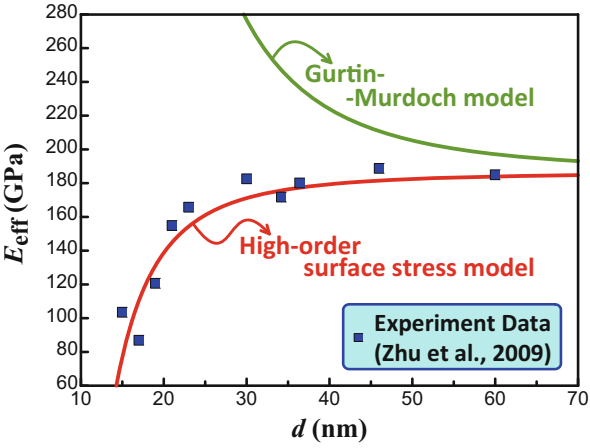


**Fig. 5.8** The size-dependent effective Young's moduli based on the high-order surface stress model and Gurtin-Murdoch model with respect to the diameter $d$ of circular NWs

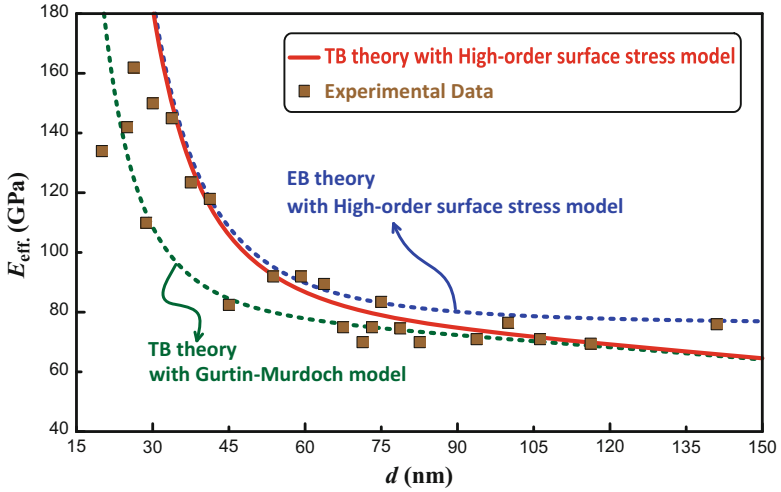


**Fig. 5.9** The difference among three continuum frameworks for the predictions on size dependence of effective Young's modulus. Note that TB theory signifies Timoshenko beam theory and EB theory denotes Euler-Bernoulli beam theory

## 5.6 Conclusions

In this chapter, we have introduced the high-order surface stress model for two-dimensional configurations. Analogous to the classical thin shell theory, this continuum theoretical framework incorporates the in-plane stresses as well as surface moments. The surface moments result in high-order surface effects. We mention that present approach to construct the high-order interface/surface conditions through the classical continuum mechanics and graphical interpretation is mathematically simple. The formulation allows that the in-plane surface stresses could be varying across the thin layer thickness and thus, effectively, it is equivalent to consider an average strain as well as curvature along the interface. In two dimensions, the behavior of interfaces can be grouped into four different types based on the degree of stiffness for the thin layer. We illustrate graphically how these four types of interfaces will influence the stress concentration factor in a successive manner for the boundary value problem of an infinite matrix containing a circular cavity.

In addition, the mechanical behaviors of NWs have been studied based on the high-order surface stress model. Both Timoshenko beam theory and Euler-Bernoulli beam theory have been adopted to incorporate the high-order surface stress effects. We compare the difference between the classical solutions (without surface effects), the calculations based on the high-order surface stress model and conventional surface stress model (Gurtin-Murdoch model). The size-dependent effective Young's modulus of NWs has also been derived. From the investigation of the theoretical calculations and the existing experimental data for the effective

Young's modulus, the effects of higher-order interface stresses between two different materials could be important, especially when the characteristic length is in a few nanometers. Our theoretical framework based on classical continuum mechanics might provide a more direct and simple approach to simulate the mechanical behavior of nanostructures.

We mention that some further studies might be envisaged for engineering applications. The thermal stress effects could be important and sensitive for nanoscaled components and structures. The issue of thermal effects on nanocomposites (Chen 1993; He and Benveniste 2004; Quang and He 2007; Chen et al. 2007b; Quang and He 2009) could be considered using the high-order interface stress model. Another possible extension of the present research can be directed to the subject of mechanics of wrinkling. Andreussi and Gurtin (1977) studied the wrinkling of a free surface and showed that a compressive residual surface tension or negative surface stiffness will result in this behavior. Kornev and Srolovitz (2004) discussed surface stress-driven wrinkling of a free film based on thermodynamics. The ordered patterns of wrinkling in metal thin films deposited on elastomeric polymer can be observed due to thermal effects (Bowden et al. 1998; Huck et al. 2000; Kwon and Lee 2005). Huang (2005) also investigated the wrinkling of a conductive thin film subjected to electric field.

Finally, we note that the high-order interface/surface stress model could be used to examine other related subjects, which have been investigated based on the Gurtin-Murdoch model, such as piezoelectric effects on nanosized structures (Chen 2008; Wang and Feng 2010; Li et al. 2011; Xiao et al. 2011; Yan and Jiang 2011a, b; Samaei et al. 2012; Yan and Jiang 2012; Hadjesfandiari 2013; Dai and Park 2013; Xiao et al. 2013), wave propagation in nanoscaled system (Gurtin and Murdoch 1976; Murdoch 1976; Chakraborty 2010; Li and Lee 2010; Ou and Lee 2012; Liu et al. 2013; Ru et al. 2013), and photonic band structures (Kushwaha et al. 1993; Chen and Wang 2011; Zhen et al. 2012; Liu et al. 2012).

**Acknowledgments** This work was supported by the Ministry of Science and Technology, Taiwan, under grant MOST 104-2221-E-006-152-MY3.

## References

Abbasion, S., Rafsanjani, A., Avazmohammadi, R., Farshidianfar, A.: Free vibration of microscaled Timoshenko beams. Appl. Phys. Lett. **95**, 143122 (2009)

Andreussi, F., Gurtin, M.E.: On the wrinkling of a free surface. J. Appl. Phys. **48**, 3798 (1977)

Assadi, A., Farshi, B., Alinia-Ziazi, A.: Size dependent dynamic analysis of nanoplates. J. Appl. Phys. **107**, 124310 (2010)

Benveniste, Y., Miloh, T.: Imperfect soft and stiff interfaces in two-dimensional elasticity. Mech. Mater. **33**, 309–323 (2001)

Benveniste, Y.: A general interface model for a three-dimensional curved thin anisotropic interphase between two anisotropic media. J. Mech. Phys. Solids. **54**, 708–734 (2006a)

Benveniste, Y.: An interface model of a three-dimensional curved interphase in conduction phenomena. Proc. R. Soc. A. **462**, 1593–1617 (2006b)

Benveniste, Y., Baum, G.: An interface model of a graded three-dimensional anisotropic curved interphase. Proc. R. Soc. A. **463**, 419–434 (2007)
Benveniste, Y., Berdichevsky, O.: On two models of arbitrarily curved three-dimensional thin interphases in elasticity. Int. J. Solids Struct. **47**, 1899–1915 (2010)
Bövik, P.: On the modeling of thin interface layers in elastic and acoustic scattering problems. Q. J. Mech. Appl. Math. **47**, 17–42 (1994)
Bowden, N., Brittain, S., Evans, A.G., Hutchinson, J.W., Whitesides, G.M.: Spontaneous formation of ordered structures in thin films of metals supported on an elastomeric polymer. Nature. **393**, 146–149 (1998)
Cammarata, R.C.: Surface and interface stress effects in thin films. Prog. Surf. Sci. **46**, 1–38 (1994)
Chakraborty, A.: The effect of surface stress on the propagation of Lamb waves. Ultrasonics. **50**, 645–649 (2010)
Chen, T.: Thermoelastic properties and conductivity of composites reinforced by spherically anisotropic particles. Mech. Mater. **14**, 257–268 (1993)
Chen, T., Dvorak, G.J.: Fibrous nanocomposites with interface stress: Hill's and Levin's connections for effective moduli. Appl. Phys. Lett. **88**, 211912 (2006)
Chen, T., Chiu, M.S., Weng, C.N.: Derivation of the generalized Young-Laplace equation of curved interface in nanoscaled solids. J. Appl. Phys. **100**, 074308 (2006)
Chen, T., Dvorak, G.J., Yu, C.C.: Size-dependent elastic properties of unidirectional nanocomposites with interface stresses. Acta Mech. **188**, 39–54 (2007a)
Chen, T., Dvorak, G.J., Yu, C.C.: Solids containing spherical nano-inclusions with interface stresses: effective properties and thermal-mechanical connections. Int. J. Solids Struct. **44**, 941–955 (2007b)
Chen, T.: Exact size-dependent connections between effective moduli of fibrous piezoelectric nanocomposites with interface effects. Acta Mech. **196**, 205–217 (2008)
Chen, A.L., Wang, Y.S.: Size-effect on band structures of nanoscale phononic crystals. Physica E. **44**, 317–321 (2011)
Chen, T., Chiu, M.S.: Effects of higher-order interface stresses on the elastic states of two-dimensional composites. Mech. Mater. **43**, 212–221 (2011)
Chiu, M.S., Chen, T.: Effects of high-order surface stress on static bending behavior of nanowires. Physica E. **44**, 714–718 (2011a)
Chiu, M.S., Chen, T.: Higher-order surface stress effects on buckling of nanowires under uniaxial compression. Procedia Eng. **10**, 397–402 (2011b)
Chiu, M.S., Chen, T.: Effects of high-order surface stress on buckling and resonance behavior of nanowires. Acta Mech. **223**, 1473–1484 (2012a)
Chiu, M.S., Chen, T.: Timoshenko beam model for buckling of nanowires with high-order surface stresses effects. Adv. Mater. Res. **528**, 281–284 (2012b)
Chiu, M.S., Chen, T.: Bending and resonance behavior of nanowires based on Timoshenko beam theory with high-order surface stress effects. Physica E. **54**, 149–156 (2013)
Dai, S., Park, H.S.: Surface effects on the piezoelectricity of ZnO nanowires. J. Mech. Phys. Solids. **61**, 385–397 (2013)
Duan, H.L., Wang, J., Huang, Z.P., Karihaloo, B.L.: Eshelby formalism for nano-inhomogeneities. Proc. R. Soc. A. **461**, 3335–3353 (2005a)
Duan, H.L., Wang, J., Huang, Z.P., Karihaloo, B.L.: Size-dependent effective elastic constants of solids containing nano-inhomogeneities with interface stress. J. Mech. Phys. Solids. **53**, 1574–1596 (2005b)
Duan, H.L., Wang, J., Huang, Z.P., Zhong, Y.: Stress fields of a spheroidal inhomogeneity with an interphase in an infinite medium under remote loadings. Proc. R. Soc. A. **461**, 1055–1080 (2005c)
Farshi, B., Assadi, A., Alinia-ziazi, A.: Frequency analysis of nanotubes with consideration of surface effects. Appl. Phys. Lett. **96**, 093105 (2010)
Gao, X.L.: A new Timoshenko beam model incorporating microstructure and surface energy effects. Acta Mech. **226**, 457–474 (2015)
Gibbs, J.W.: The Collected Works of J. W. Gibbs, vol. 1. Longman, New York (1928)

Gurtin, M.E., Murdoch, A.I.: A continuum theory of elastic material surfaces. Arch. Ration. Mech. Anal. **57**, 291–323 (1975)
Gurtin, M.E., Murdoch, A.I.: Effect of surface stress on wave propagation in solids. J. Appl. Phys. **47**, 4414 (1976)
Gurtin, M.E., Murdoch, A.I.: Surface stress in solids. Int. J. Solids Struct. **14**, 431–440 (1978)
Gurtin, M.E., Weissmüller, J., Larché, F.: A general theory of curved deformable interfaces in solids at equilibrium. Philos. Mag. A. **78**, 1093–1109 (1998)
Hadjesfandiari, A.R.: Size-dependent piezoelectricity. Int. J. Solids Struct. **50**, 2781–2791 (2013)
He, Q.C., Benveniste, Y.: Exactly solvable spherically anisotropic thermoelastic microstructures. J. Mech. Phys. Solids. **52**, 2661–2682 (2004)
He, J., Lilley, C.M.: Surface effect on the elastic behavior of static bending nanowires. Nano Lett. **8**, 1798–1802 (2008a)
He, J., Lilley, C.M.: Surface stress effect on bending resonance of nanowires with different boundary conditions. Appl. Phys. Lett. **93**, 263108 (2008b)
He, Q., Lilley, C.M.: Resonant frequency analysis of Timoshenko nanowires with surface stress for different boundary conditions. Appl. Phys. Lett. **112**, 074322 (2012)
Hill, R.: Theory of mechanical properties of fibre-strengthened materials: I. Elastic behaviour. J. Mech. Phys. Solids **12**, 199–212 (1964)
Huang, R.: Electrically induced surface instability of a conductive thin film on a dielectric substrate. Appl. Phys. Lett. **87**, 151911 (2005)
Huck, W.T.S., Bowden, N., Onck, P., Pardoen, T., Hutchinson, J.W., Whitesides, G.M.: Ordering of spontaneously formed buckles on planar surfaces. Langmuir. **16**, 3497–3501 (2000)
Ji, L.W., Young, S.J., Fang, T.H., Liu, C.H.: Buckling characterization of vertical ZnO nanowires using nanoindentation. Appl. Phys. Lett. **90**, 033109 (2007)
Jiang, L.Y., Yan, Z.: Timoshenko beam model for static bending of nanowires with surface effects. Physica E. **42**, 2274–2279 (2010)
Jing, G.Y., Duan, H.L., Sun, X.M., Zhang, Z.S., Xu, J., Li, Y.D., Wang, X.J., Yu, D.P.: Surface effects on elastic properties of silver nanowires: contact atomic-force microscopy. Phys. Rev. B. **73**, 235409 (2006)
Kornev, K.G., Srolovitz, D.J.: Surface stress-driven instabilities of a free film. Appl. Phys. Lett. **85**, 2487–2489 (2004)
Kushwaha, M.S., Halevi, P., Dobrzynski, L., Djafari-Rouhani, B.: Acoustic band structure of periodic elastic composites. Phys. Rev. Lett. **71**, 2022–2025 (1993)
Kwon, S.J., Lee, H.H.: Theoretical analysis of two-dimensional buckling patterns of thin metal-polymer bilayer on the substrate. J. Appl. Phys. **98**, 063526 (2005)
Lachut, M.J., Sader, J.E.: Effect of surface stress on the stiffness of cantilever plates. Phys. Rev. Lett. **99**, 206102 (2007)
Laplace, P.S.: Traite de mechanique celeste; supplements au Livre X. Euvres Complete Vol. 4. Gauthier-Villars, Paris (1806)
Landau, L.D., Lifshitz, E.M.: Fluid Mechanic, 2nd edn. Pergamon Press, Oxford (1987)
Li, Y., Fang, B., Zhang, J., Song, J.: Surface effects on the wrinkling of piezoelectric films on compliant substrates. J. Appl. Phys. **110**, 114303 (2011)
Li, Y.D., Lee, K.Y.: Size-dependent behavior of Love wave propagation in a nanocoating. Mod. Phys. Lett. B. **24**, 3015–3023 (2010)
Liu, W., Chen, J.W., Liu, Y.Q., Su, X.Y.: Effect of interface/surface stress on the elastic wave band structure of two-dimensional phononic crystals. Phys. Lett. A. **376**, 605–609 (2012)
Liu, H., Liu, H., Yang, J.: Surface effects on the propagation of shear horizontal waves in thin films with nano-scalethickness. Physica E. **49**, 13–17 (2013)
Miller, R.E., Shenoy, V.B.: Size-dependent elastic properties of nanosized structural elements. Nanotechnology. **11**, 139–147 (2000)
Murdoch, A.I.: The propagation of surface waves in bodies with material boundaries. J. Mech. Phys. Solids. **24**, 137–146 (1976)
Ni, H., Li, X.: Young's modulus of ZnO nanobelts measured using atomic force microscopy and nanoindentation techniques. Nanotechnology. **17**, 3591–3597 (2006)

Nix, W.D., Gao, H.: An atomistic interpretation of interface stress. Scr. Mater. **39**, 1653–1661 (1998)
Ou, Z.Y., Lee, D.W.: Effects of interface energy on scattering of plane elastic wave by a nano-sized coated fiber. J. Sound Vib. **331**, 5623–5643 (2012)
Povstenko, Y.Z.: Theoretical investigation of phenomena caused by heterogeneous surface tension in solids. J. Mech. Phys. Solids. **41**, 1499–1514 (1993)
Quang, H.L., He, Q.C.: Size-dependent effective thermoelastic properties of nanocomposites with spherically anisotropic phases. J. Mech. Phys. Solids. **55**, 1889–1921 (2007)
Quang, H.L., He, Q.C.: Estimation of the effective thermoelastic moduli of fibrous nanocomposites with cylindrically anisotropic phases. Arch. Appl. Mech. **79**, 225–248 (2009)
Ru, C.Q.: Simple geometrical explanation of Gurtin-Murdoch model of surface elasticity with clarification of its related versions. Sci. China. **53**, 536–544 (2010)
Ru, Y., Wang, G.F., Su, L.C., Wang, T.J.: Scattering of vertical shear waves by a cluster of nanosized cylindrical holes with surface effect. Acta Mech. **224**, 935–944 (2013)
Samaei, A.T., Bakhtiari, M., Wang, G.F.: Timoshenko beam model for buckling of piezoelectric nanowires with surface effects. Nanoscale Res. Lett. **7**, 201 (2012)
Sharma, P., Ganti, S., Bhate, N.: Effect of surfaces on the size-dependent elastic state of nano-inhomogeneities. Appl. Phys. Lett. **82**, 535–537 (2003)
Sharma, P., Ganti, S.: Size-dependent Eshelby's tensor for embedded nano-inclusions incorporating surface/interface energies. J. Appl. Mech. **71**, 663–671 (2004)
Shuttleworth, R.: The surface tension of solids. Proc. Phys. Soc. A. **63**, 444–457 (1950)
Song, J., Wang, X., Riedo, E., Wang, Z.L.: Elastic property of vertically aligned nanowires. Nano Lett. **5**, 1954–1958 (2005)
Spaepen, F.: Interfaces and stresses in thin films. Acta Mater. **48**, 31–42 (2000)
Ting, T.C.T.: Mechanics of a thin anisotropic elastic layer and a layer that is bonded to an anisotropic elastic body or bodies. Proc. R. Soc. A. **463**, 2223–2239 (2007)
Timoshenko, S.P., Gere, J.M.: Theory of Elastic Stability. McGraw-Hill, New York (1961)
Timoshenko, S.P., Goodier, J.N.: Theory of Elasticity. McGraw-Hill, New York (1970)
Thomson, R., Chuang, T.J., Lin, I.H.: The role of surface stress in fracture. Acat Metall. **34**, 1133–1143 (1986)
Wang, Z.L.: ZnO nanowire and nanobelt platform for nanotechnology. Mater. Sci. Eng.: Rep. **64**, 33–71 (2009)
Wang, G.F., Feng, X.Q.: Effects of surface elasticity and residual surface tension on the natural frequency of microbeams. Appl. Phys. Lett. **90**, 231904 (2007)
Wang, G.F., Feng, X.Q.: Surface effects on buckling of nanowires under uniaxial compression. Appl. Phys. Lett. **94**, 141913 (2009a)
Wang, G.F., Feng, X.Q.: Timoshenko beam model for buckling and vibration of nanowires with surface effects. J. Phys. D: Appl. Phys. **42**, 155411 (2009b)
Wang, G.F., Feng, X.Q.: Effect of surface stresses on the vibration and buckling of piezoelectric nanowires. Europhys. Lett. **91**, 56007 (2010)
Wang, D.H., Wang, G.F.: Surface effects on the vibration and buckling of double-nanobeam-systems. J. Nanomater. **2011**, 518706 (2011)
Wang, G.F., Yang, F.: Postbuckling analysis of nanowires with surface effects. J. Appl. Phys. **109**, 063535 (2011)
Weng, C.N., Chen, T.: General interface conditions in surface elasticity of nanoscaled solids in general curvilinear coordinates. J. Mech. **26**, 81–86 (2010). doi:10.1017/S1727719100003749
Xiao, J.H., Xu, Y.L., Zhang, F.C.: Size-dependent effective electroelastic moduli of piezoelectric nanocomposites with interface effect. Acta Mech. **222**, 59–67 (2011)
Xiao, J.H., Xu, Y.L., Zhang, F.C.: Evaluation of effective electroelastic properties of piezoelectric coated nano-inclusion composites with interface effect under antiplane shear. Int. J. Eng. Sci. **69**, 61–68 (2013)
Yan, Z., Jiang, L.Y.: The vibrational and buckling behaviors of piezoelectric nanobeams with surface effects. Nanotechnology. **22**, 245703 (2011a)

Yan, Z., Jiang, L.Y.: Surface effects on the electromechanical coupling and bending behaviours of piezoelectric nanowires. J. Phys. D: Appl. Phys. **44**, 075404 (2011b)

Yan, Z., Jiang, L.Y.: Vibration and buckling analysis of a piezoelectric nanoplate considering surface effects and in-plane constraints. Proc. R. Soc. A. **468**, 3458–3475 (2012)

Young, T.: Phil.: an essay on the cohesion of fluid. Philos. Trans. R. Soc. Lond. **95**, 65–87 (1805)

Young, S.J., Ji, L.W., Chang, S.J., Fang, T.H., Hsueh, T.J., Meen, T.H., Chen, I.C.: Nanoscale mechanical characteristics of vertical ZnO nanowires grown on ZnO: Ga/glass templates. Nanotechnology. **18**, 225603 (2007)

Zhang, Y., Zhuo, L.J., Zhao, H.S.: Determining the effects of surface elasticity and surface stress by measuring the shifts of resonant frequencies. Proc. R. Soc. A. **469**, 20130449 (2013)

Zhen, N., Wang, Y.S., Zhang, C.Z.: Surface/interface effect on band structures of nanosized phononic crystals. Mech. Res. Commun. **46**, 81–89 (2012)

Zhou, L.G., Huang, H.C.: Are surfaces elastically softer or stiffer? Appl. Phys. Lett. **84**, 1940–1942 (2004)

Zhu, Y., Xu, F., Qin, Q., Fung, W.Y., Lu, W.: Mechanical properties of vapor-liquid-solid synthesized silicon nanowires. Nano Lett. **9**, 3934–3939 (2009)